



Ship Longitudinal Strength Modeling for Reliability Analysis

P.A. Frieze, Paul A. Frieze & Associates, Twickenham, United Kingdom
Y-T Lin, National Taiwan Ocean University, Taiwan, Republic of China

ABSTRACT

A numerical procedure for the evaluation of ship longitudinal bending strength is described. It accounts directly for all the relevant destabilising parameters involved, material properties, geometry, and fabrication defects. Simulations of experimental results on steel box girder models are used to demonstrate its accuracy.

Based on the observation that ship bending strength closely correlates with the strength of the critical stiffened panel of a girder's cross-section, a simplified hull strength model is developed. The model accounts explicitly for the material, and plate and stiffened panel slendernesses, and implicitly for plate and stiffened panel initial deflections and welding residual stresses. Representative values for the latter were selected following the analysis of a range of typical stiffened plate configurations.

The simplified hull girder model is subject to reliability analysis to help identify the important parameters, loading and resistance, affecting hull lifetime reliability.

NOMENCLATURE

a	plate length
A	cross-sectional area
b	plate width
B	width of angle stiffener table
C_s	block coefficient
d	overall stiffener depth
D	hull depth
E	Young's modulus
H	neutral axis to extreme fibre dist.
I	moment of inertia
L	stiffened panel length
M	moment
r	radius of gyration
S_f	shape factor
t	plate thickness
V	Froude number
Z	section modulus
α_1	A_1/A
β	$=(b/t)(\sigma_y/E)^{1/2}$ =plate slenderness

γ	H_b/D
δ_0	plate initial deflection
Δ	stiffener initial deflection
ϵ	strain
λ	$= (L/\pi r)(\sigma_y/E)^{1/2}$ =stiffened panel slenderness
ηt	width of weld tensile yield zone
ϕ	stiffened panel strength ratio
χ	modelling uncertainty
ψ_s	combination coefficient to account for correlation between wave and still water bending moments
σ	stress
θ	heading (180° equates to head seas)
θ	hull curvature
θ_c	end of stable curvature range

Superscripts

' normalised w.r.t. yield value

Subscripts

B	girder bottom
D	deck
e	effective
MC	measured v calculated
p	plastic
Q	extreme fibre
r	residual stress
sw	still water
S	side-shell
u	ultimate
w	wave
Y	yield

INTRODUCTION

Ship rules are traditionally expressed in a form which has little to do with their structural strength. The very complex loading patterns to which ships are subjected - still water loads, and sea states the effects of which can be modified by operator intervention - have had a significant influence on the growth of these.

With the demand for risk assessment for many types of ships now in place, the need for a formal framework for the safety evaluation of ships has developed. Structural reliability analysis provides one such framework but requires the development of simple yet accurate methodologies for the ultimate strength evaluation of ships structures and their components if it is to be efficiently and effectively exploited.

This paper is concerned with the development of a numerical procedure for the determination of overall hull girder strength and which includes consideration of the parameters that contribute to this through buckling and yielding. The purpose of this is to provide a basis for the derivation of a model which also accounts for these parameters but in a simplified form amenable to reliability modelling.

The basis for the numerical model is described and its accuracy substantiated against tests on steel box girders representative of simple ship structures. Following this, the simplified model is established and its accuracy quantified against the experimental data. The model is then used in the reliability analysis of a ships hull as part of the ISSC'91 Committee V.1 work.

HULL GIRDER MODELLING

Background

From the point of view of structural analysis, the failure of a ship's hull girder subjected to vertical bending moment may be due to brittle fracture, fatigue fracture, yielding, spreading of plasticity, instability, or a combination of these events. It may fail gradually as in the case of a lengthening fatigue crack or spreading plasticity, or suddenly through plastic instability or propagation of a brittle crack [1].

Although initial yield, which occurs at some points in a structure, does not necessarily cause direct failure, the spreading of plastic deformation over a substantial portion of a structure may lead to structural failure. In the case of a hull girder, yielding generally commences in the deck or bottom structure and spreads towards side shells as the applied vertical bending moment is increased. Ultimately, a fully plastic moment is reached when yield has developed at every point throughout the girder depth [2]. This moment represents an upper limit of a girder's longitudinal strength, but will rarely be attained due to the adverse effects of buckling of the longitudinal structure between frames, of weld-induced residual stresses, or of initial deformations resulting from fabrication. In the practical case, failure is influenced by buckling or

yielding of the compression flange and yielding of the tension flange.

When a structural member is subjected to compression, buckling may occur at stress levels well below the yield strength. This type of instability failure is characterised by a relatively rapid increase in deflection for a small increase in load as the compressive stress approaches a critical value. For a hull girder under vertical bending moment, buckling does not immediately result in complete collapse of the girder. The post-buckling behaviour depends on the detailed structural arrangement. In transversely framed ships, the plating buckles between frames so the reserve strength after buckling may be small. In longitudinally framed ships, however, the plating after buckling between longitudinals, redistributes its load to adjacent stiffened panels and the plate-stiffener combination can carry further loading until it buckles between transverse supporting members. As a result, the maximum load-carrying capacity of longitudinally framed vessels may be significantly greater than the load at which buckling commences.

The possible collapse modes for a stiffened panel under axial compression are:

- (a) Flexural buckling induced by plate failure: this mode involves buckling towards the stiffener outstand and is precipitated by loss of compressive strength and stiffness of the plate.
- (b) Flexural buckling induced by stiffener yield failure: in this case collapse occurs in the direction away from the stiffener outstand.
- (c) Torsional tripping of the stiffener: this mode can occur in panels with torsionally weak stiffeners.
- (d) Overall grillage buckling: this involves buckling of the transverse as well as longitudinal stiffeners.

Torsional buckling is usually avoided by providing sufficiently stocky stiffeners or tripping brackets, and suppression of overall buckling can be achieved by the use of stiff transverse supporting members. The major problem facing a designer is interframe flexural buckling in modes induced either by plate or stiffener failure.

Discretisation

As indicated, failure of an individual structural element, either precipitated by yielding or buckling, does not necessarily imply failure of the entire girder. Failure of a number of structural elements, however, does result in collapse of the hull. This may occur in two different ways: (1) collapse caused by a series of failures of structural elements, and (2) simultaneous

overall instability of the complete cross-section.

Fortunately, except for the overall grillage buckling, the ductile collapse of a ship's hull girder is most probably due to a sequence rather than a coincidence of failures of structural elements. This enables one to divide the midship section into structural elements which respond to the imposed loads independently, and to concentrate on their collapse behaviour. The types of structural elements considered in the present study include the stiffened panel, the plate element and the hard corner, which are now discussed in turn.

Stiffened Panel

This element, which is typically found in longitudinally framed structures, is composed of a stiffener and attached plate. The plate ranges from the midpoint of a plate panel between two longitudinal stiffeners to the midpoint of the adjacent plate panel. The stiffener may be a flat-bar, a T-section or an angle bar. The behaviour of stiffened panels under compression can conveniently be represented by load-end shortening curves, i.e. average stress-strain curves. A computer program [3] was used to generate the load-end shortening curves for stiffened panels which make up the cross-section of a hull or box girder. The extent of the analysis was from mid-span of one panel to mid-span of an adjacent panel. This approach by-passed the problem of identifying which mode (plate- or stiffener-induced) precipitated failure. The analysis allowed different levels of initial stiffener deflection to be considered in each half span.

The parameters which affect the compressive behaviour of stiffened panels include plate slenderness, weld-induced residual stress in the plate, maximum initial deformation in the plate, column slenderness of the stiffened panel, initial stiffener bow, and material properties. The effects of all these parameters are accounted for by the use of load-end shortening curves. In a longitudinally framed hull girder, the midship section usually comprises fifty or more stiffened panels, which may differ in geometry, material property or location in the cross-section. Since parts of these panels exhibit virtually the same collapse behaviour, it is uneconomical to generate the average compressive stress-strain curve for every stiffened panel forming the cross-section. Stiffened panels are thus divided into groups of panels with nearly identical parameters. A representative panel within each group is selected, based on engineering judgment, for generating the load-shortening curve.

Plate Element

This kind of structural element comprises a single plate only and is defined by its thickness and the coordinates of the plate edges. There are two possible ways in which plate panels may be found in box or hull girders. Firstly, 'wide plate' elements are created in transversely framed panels. Secondly, 'long plate' elements are present in longitudinally framed structures where a plate-stiffener combination is so stocky that interframe flexural buckling is precluded and only the effect of plate buckling has to be allowed for.

The elasto-plastic buckling behaviour of wide plate elements under longitudinal compression is basically equivalent to the behaviour of long plates under transverse compression which can be appropriately covered by average stress-strain curves. Numerical studies [4,5] provide a useful basis for the evaluation of the stiffness and strength of long plates in transverse compression, which are strongly influenced by plate slenderness, aspect ratio and level of weld-induced imperfections. Typical average stress-strain curves derived from [4] are illustrated in Fig 1.

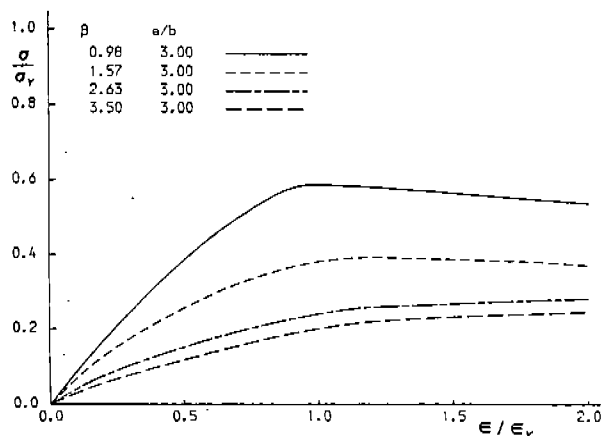


Fig. 1 Average Stress-Strain Curves for Plates in Transverse Compression

The compressive behaviour of long plates has similarly been examined using numerical procedures [6,7]. To simplify and generalise the extensive elasto-plastic buckling results of [6], [3] developed a parameterised model which could efficiently determine the stress level in a plate given the extent of compressive strain, the plate slenderness, and the level of weld-induced imperfections. This same model was used in [3] in the derivation of interframe buckling stress-strain curves.

The tensile behaviour of plates is mainly influenced by the magnitude of

weld-induced residual stress. For stress-free plates it is appropriate to suppose that the plates follow the material stress-strain curve. For plates with weld-induced residual stress, however, initial stiffness is factored due to the yielding tension blocks by the amount:

$$1 - \frac{2\eta t}{b} = \frac{1}{1 + \sigma_r'} \quad (1)$$

If a linear relationship is assumed up to the point where yielding occurs in the pre-compression zone, the non-dimensional strain corresponding to this point is:

$$\epsilon'_m = 1 + \sigma_r' \quad (2)$$

If a parabola is assumed to represent the response over the strain range

$$1 \leq \epsilon' < 1 + 2\sigma_r'$$

it can be expressed by

$$\sigma' = \frac{1}{4\sigma_r'(1+\sigma_r')} [-\epsilon'^2 + (2+4\sigma_r')\epsilon' - 1] \quad (3)$$

and is connected to the neighbouring linear sections with appropriate slopes. This form of representation accounts for the adverse effects of initial deformation and residual stress.

Hard Corner

At certain locations of a hull cross-section, the local structure is strengthened by the connecting members in such a rigid way that it is reasonable to assume that the structure can sustain the imposed compressive load up to the yield point and beyond without suffering any form of instability. That is, it effectively follows the material stress-strain curve over the full loading range. These regions, called 'hard corners' [8], include deck stringers, shear strakes, intersections of deck plating with deep girders and longitudinal bulkheads, intersections of shell plating with superstructure, bilge keels, deep girders, longitudinal bulkheads and keel, etc.

The geometry of hard corners can be described in two different ways. Firstly, a hard corner composed of several interconnecting plates is treated as a group of plate elements and defined by the thicknesses and locations of plate elements. Secondly, the area, centroid and moment of inertia of the cross-section of a hard corner are calculated manually and input directly. This format allows a number of interconnecting plates to be described as a single hard corner element.

NUMERICAL PROCEDURE

Assumptions

The assumptions made in predicting the hull girder response to extreme vertical bending moment are:

1. Plane cross-sections of the hull girder before bending remain plane after any load application, thus the distribution of strain over the cross-section is linear.

2. The midship section of the hull girder is discretised into a set of structural elements of which the height is sufficiently small compared with the ship's depth that a uniform strain distribution can be assumed to act over the cross-section of each element. The uniform strain acting on the cross-section of a structural element is taken as the value of the linearly distributed strain at the centroid of the cross-section (Fig. 2).

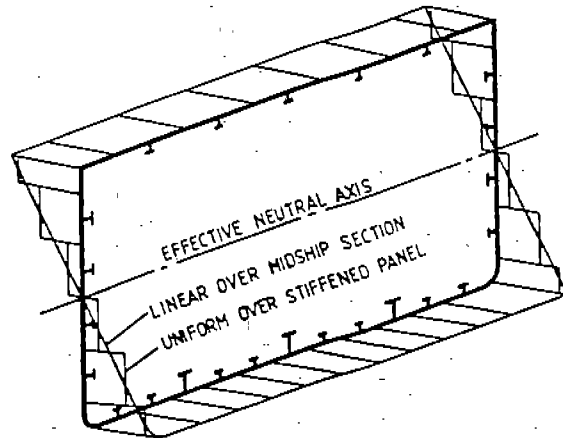


Fig. 2 Assumed Cross-Section Strain Distribution

3. The stress-strain relationship for either long or wide plate elements in compression is appropriately represented by average stress-strain curves derived from the large deflection elasto-plastic analysis of the isolated plate panels simplified as described in [3].

4. The elasto-plastic behaviour of stiffened panels in compression is described by load-end shortening curves which are specifically derived using the procedure developed in [3].

5. The hard corner behaviour is defined by the material stress-strain curve.

6. Since shear forces are generally small at the midship section, the effect of shear stress on yielding is neglected.

7. Neither fatigue nor ductile fracture modes of failure are considered.

8. Since ultimate hull girder collapse occurs in most cases before outer-fibre strains reach two times yield strain, and for shipbuilding steels strain hardening does not occur until strain exceeds yield strain by eight to ten times, the material itself is taken to behave elastic-perfectly plastic in tension and compression.

Application of Load Increments

Loading is applied to the hull girder in the form of curvature instead of bending moment. Since a linear strain distribution over the mid-section is assumed, the strain at the centroids of structural elements caused by the imposed curvature can be determined on the basis of the mid-section's effective neutral axis. The corresponding stress acting on each structural element is then calculated from its average stress-strain curve using interpolation if necessary. Although strain is assumed to be distributed linearly over the section, stress varies non-linearly due to the effects of fabrication-induced distortions, weld-induced residual stress and buckling. Finally, the bending moment acting on the hull girder is computed for the applied curvature by summing the contributions from all of the structural elements. After this procedure has been repeated for increasing levels of curvature, pairs of data of bending moments and curvatures can be obtained to plot the bending moment-curvature curve which includes the maximum bending moment and the pre- and post-collapse behaviour of the hull girder.

Since the curvature at which collapse of a girder occurs varies to a high degree with the magnitude of the ship's height, it is appropriate to express the curvature increments in a form non-dimensionalised with respect to

$$\theta_y = \frac{\epsilon_{y0}}{H} = \frac{\sigma_{y0}}{E_y H} \quad (4)$$

Location of Effective Neutral Axis

The location of the plane of zero strain, the 'effective neutral axis', for an applied curvature is determined by the state of stress existing in the structural elements forming the midship section. As the applied loading is increased, the effective neutral axis shifts towards the tension flange due to loss of stiffness of the structural elements in the compression zone. At each value of curvature, location of the effective neutral axis is determined on the condition that the sum of the axial forces carried by all of the structural elements equals zero.

The state of stress of a structural element is connected with a particular value of strain through the element's average stress-strain curve, while the strain itself is proportional to the distance between the centroid of the structural element and the effective neutral axis. Therefore, the location of the effective neutral axis must be iteratively determined from the condition

of equilibrium. The algorithm employed is described in detail in [3].

Evaluation of Bending Moment

After the location of the effective neutral axis is determined for a particular curvature increment, the corresponding incremental bending moment can be evaluated. This is obtained by summing the contributions from all the elements that make up the mid-section. The moment and curvature are then non-dimensionalised with respect to M_y and the first yield curvature.

The fully plastic moment of a ship girder, which represents an upper limit of its load-carrying capacity as a beam, is readily calculable based on the plastic hinge concept [2]. Following the method of classical plasticity, the ultimate limit condition is reached when yield occurs at every point of the cross-section. In this case, the 'plastic neutral axis' coincides with the interface which divides the cross-section into two regions with equal 'squash' loads in tension and compression.

The first yield curvature and the corresponding bending moment M_y of a ship's girder can be determined by the standard section modulus calculation. First the location of the 'elastic neutral axis' is determined for the fully effective mid-section. Then θ_y is given by eqn (4) and M_y can be evaluated from:

$$M_y = \sigma_{y0} I / H \quad (5)$$

Bending Moment-Curvature Curve

Curvature of the hull girder axis is considered to be positive when the hull girder is bent concave upwards and negative when concave downwards, i.e. positive in sagging and negative in hogging. Similarly the bending moment is positive when it produces compression in the deck and tension in the bottom.

Using the numerical procedure discussed above, it is therefore possible to obtain a particular bending moment increment for any curvature increment imposed on a girder. If this procedure is repeatedly carried out for increasing levels of curvature, the non-dimensional bending moment-curvature curve is generated. Separate runs are performed for the hull girder in sagging and hogging to provide the complete history of the girder under vertical bending.

Typical moment-curvature curves are shown in Fig. 3. The full range of behaviour in either sagging or hogging can be divided into three zones of behaviour. The first depicts stable behaviour in which the curvature imposed

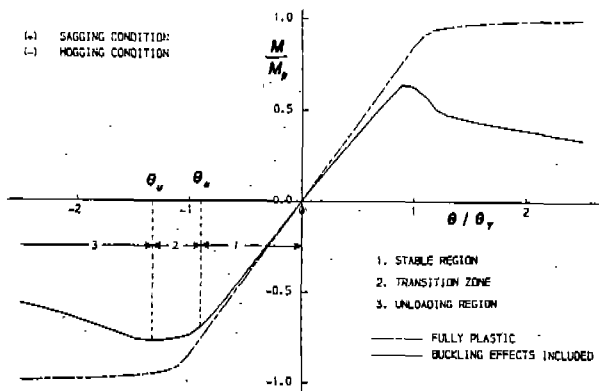


Fig. 3 Typical Hull Bending Moment-Curvature Behaviour

on the hull girder is less than a critical value θ_c which is the smaller of the curvatures to first yield or to the buckling of some major components. If the effects of neither buckling nor yielding are significant, the curve in this region is virtually linear. The slope of the bending moment-curvature curve, however, commences to decrease noticeably from the curvature θ_c and decreases until it eventually approaches zero at the curvature θ_u at which peak moment occurs. The second zone, i.e. the transition zone, ranges from θ_c to θ_u . The third zone occurs beyond θ_u and is characterised by negative slopes, i.e. the load-carrying capacity of the girder reduces with increasing curvature.

Collapse behaviour of hull girders mainly differs in the last two zones and is influenced by such factors as material properties, geometric configurations, initial imperfections, degree of structural redundancy, etc. For a girder with little redundancy, collapse is usually precipitated by failure of a significant portion of the structure, leading to a sudden drop in bending moment capacity after reaching the critical curvature. The second zone, therefore, lasts for a relatively short range in this case. In contrast, for a girder with greater redundancy, collapse occurs gradually as a result of the successive failure of smaller portions of the structure. That is, the load shed by some components due to their failure can be carried by the reserve load-carrying capacity of neighbouring elements. Thus, final collapse of the whole mid-section is delayed by this load redistribution, which results in a longer transition zone.

When all the structural elements forming the mid-section of a hull girder are assumed to follow the material stress-strain curve both in tension and

compression, a bending moment-curvature curve can be generated for the fully effective cross-section (Fig. 3). Since effects of structural instability are excluded in this idealised case, bending failure can occur through material yielding only. As the accumulative curvature is increased, yielding begins at the outermost fibre of the deck or bottom structure, and then spreads gradually down or up the side shells. The curve thus approaches asymptotically a horizontal line determined by the fully plastic moment. Comparing this fully effective curve with a realistic bending moment-curvature curve, the difference that is attributable to buckling effects can clearly be identified.

HULL GIRDER STUDY

Introduction

Using the above procedure, the response of a number of box and hull girder sections has been examined [3]. This concentrated on sections which had been tested experimentally and simulated numerically in order to substantiate the procedure but also included additional analyses to investigate aspects such as stiffening configurations. These were executed so that the results could be generalised and simplified for use in reliability modelling as described later. The results considered concern:-

* Box girders Models 2 and 4, which were tested at Imperial College under pure bending conditions and failed by buckling of the stiffened compression flange panels [9,10]. The effects of initial stiffener deflections, behaviour of hard corners and residual stresses contained in the tension flange on the behaviour of the girders were specifically examined.

* Box girders Models 23 and 31, tested by Reckling [11] for which variation of the ultimate strengths of the girders with differing welding residual stresses and initial imperfections were considered.

* Two transversely framed warships, T.B.D. COBRA and T.B.D. WOLF based on numerical results obtained by Faulkner et al [12].

Box Girder Models 2 and 4 [9,10]

Both models were subjected to pure bending and failed by buckling of the stiffened compression flange panels. Model 8 of the same series was also tested in pure bending. It suffered orthotropic buckling of the compression flange, however, so was not readily amenable for comparison using the present approach.

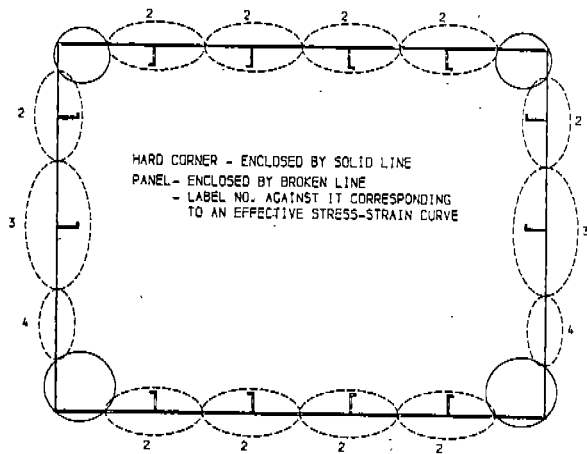


Fig. 4 Discretisation of Model 2 [13,14]

Model 2. The cross-section of Model 2 [13,14] was discretised into structural elements, i.e. stiffened panels, plate elements and hard corners, as shown in Fig. 4. The component dimensions and material properties are as listed in Table 1. The hard corners were assumed to have an elastic-perfectly plastic relationship in both tension and compression.

In the first test on Model 2 (Test 2A), collapse was precipitated by plate buckling at one end of the box probably due to the high transverse residual stress occurring near the diaphragm [14]. After stiffening of the end bays the box was tested again (Test 2B) and collapse occurred at an internal section, but the maximum load was exactly the same as in Test 2A. Residual stresses and initial imperfections were measured before each of these two tests, those for the second test clearly including those resulting from the first test. These are listed in Table 2 and were used in the present study to analyse the overall behaviour of the girder. The average stress-strain curves for plate panels in the compression flange and webs were derived by the simplified method and are shown in

Table 1
Component Dimensions and Material Properties of Models 2 and 4 [9,10] and Models 23 and 31 [11]

	Model 2	Model 4	Model 23	Model 31
<u>Compression Flange Plate</u>				
b	241.30	120.65	85.71	120.00
t	4.864	5.017	2.50	2.50
σ_y	297.3	221.0	246.0	255.0
E	208,500	207,000	210,000	210,000
<u>Tension Flange Plate</u>				
b	241.30	120.65	85.71	120.00
t	4.864	4.943	2.50	2.50
σ_y	297.3	215.6	246.0	255.0
E	208,500	208,700	210,000	210,000
<u>Web Plate</u>				
b	273.05	98.425	100.00	133.33
	-	114.30	-	-
	-	111.125	-	-
t	3.366	4.943	2.50	2.50
σ_y	211.9	280.6	246.0	255.0
E	216,200	214,100	210,000	210,000
<u>Stiffener (angle)</u>				
d	50.80	50.80	30.00	30.00
B	15.875	15.875	20.00	20.00
t	4.763	4.763	2.50	2.50
σ_y	276.2	287.9	246.0	255.0
E	191,500	199,200	210,000	210,000
<u>Stiffener (flat)</u>				
d	-	50.80	30.00	30.00
t	-	6.35	2.50	2.50
σ_y	-	303.8	246.0	255.0
E	-	206,200	210,000	210,000
<u>Mid-section particulars</u>				
A	21554	29144	6875.0	6250.0
I	3411.8	4331.6	197.44	180.35
H_b	465.10	468.8	200.00	200.00
M_p	2243.3	2626.9	268.20	253.65

Units: Length in mm; Area in mm²; Inertia in m² mm²; Stress in N/mm²; Moment in kNm.

Fig. 5 for Test 2A. These curves were used in the large deflection elasto-plastic analysis of the double-span stiffened panels with residual stresses and initial imperfections as listed in Table 2. The Test 2A computed load-

Table 2
Initial Imperfections and Comparisons between Numerical and Test Results for Girder Models 2 and 4 [9,10]

	Model 2		Model 4			Corner Model Type A	Model Type B	Res. Stress in Tens. Fl.
	Test 2A	Test 2B	Initial Mode 1	Stiff. Mode 2	Deflns Mode 3			
σ_r	0.176	0.176	0.562	0.562	0.562	0.562	0.562	0.562
δ_o / b	1/400	1/100	1/800	1/800	1/800	1/800	1/800	1/800
Δ / L	-1/1450	1/580	-1/1050	-1/660	-1/510	-1/510	-1/510	-1/510
M_u (kNm) (num.)	1/2280	1/1430	1/1950	1/4920	1/510	1/510	1/510	1/510
M_u / M_p (num.)	1620	1471	2421	2418	2344	2322	2324	2421
M_u (kNm) (expt)	0.722	0.656	0.921	0.920	0.892	0.884	0.885	0.882
M_u / M_p (expt)	1543	1543	2212	2212	2212	2212	2212	2212
M_u / M_p (expt)	0.688	0.688	0.842	0.842	0.842	0.842	0.842	0.842

Notes 1. Corner behaviour is represented by material stress-strain curve.
2. Unless noted, effects of residual stresses in tension flange are ignored.

shortening curves for the stiffened panels in the compression flange and the webs are shown in Fig. 6.

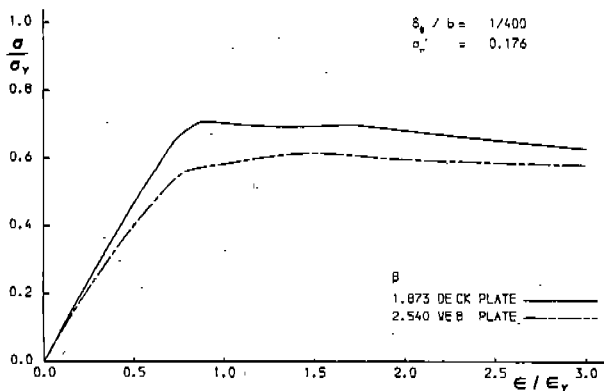


Fig. 5 Plate Average Stress-Strain Curves for Model 2 - Test 2A

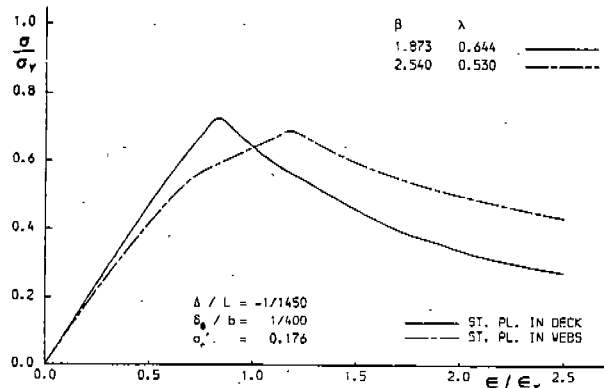


Fig. 6 Stiffened Plate Load-Shortening Curves for Model 2 - Test 2A

The pure bending tests on Model 2 were carried out in the sagging condition. Therefore, the bending moment-curvature relationships were computed using the present method for the sagging condition only. They are plotted in Fig. 7 together with the experimental result [15] and the fully plastic response in both sagging and hogging. Comparisons between the predicted and experimental results are also presented

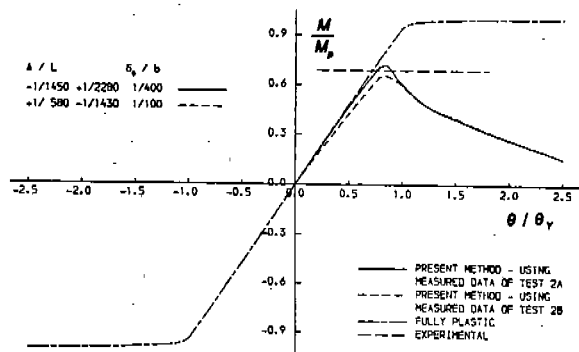


Fig. 7 Bending-Moment Curvature Response for Model 2

in Table 2. The agreement is seen to be satisfactory with the predicted maximum bending moment being 4.9% higher than the collapse moment in Test 2A and 4.6% lower than in Test 2B.

Model 4. Box girder Model 4 [16,17] had the same overall dimensions as Model 2 but more closely spaced stiffeners. Similarly to Model 2, the cross-section of Model 4 was discretised into structural elements including stiffened panels, plate elements and hard corners. Component dimensions and material properties are listed in Table 1.

As illustrated in Fig. 6, the stiffness and load-carrying capacity of stiffened panels are dependent upon the magnitudes of the weld-induced residual stress and initial imperfections, in addition to such parameters as plate slenderness and column slenderness. Consequently, maximum bending moment and collapse behaviour of box girders incorporating such members are similarly influenced. Therefore, where initial imperfections and residual stresses in panels vary, it is necessary when using one stiffened panel load-shortening curve to represent the panel behaviour that this should be representative of the entire panel, and not just the maximum, for example.

Thus three combinations of initial imperfections were selected from the measurements [17] for analysis: they are listed in Table 2. One average residual stress level in the plate and one maximum initial plate deflection were used throughout, while three different levels of maximum initial stiffener deflection in two consecutive spans were adopted. The deflections correspond to the most severely deformed (Mode 3) condition and to two slightly deformed shapes (Modes 1 and 2). The load-shortening curves for the stiffened panels in both the compression flange and the webs with the three combinations of initial imperfections were computed [3]. By incorporating these load-shortening curves as the effective stress-strain curves in the present incremental moment-curvature analysis, the sagging bending moment-curvature relationships were obtained.

Mode 3 represented the largest measured values of the initial stiffener deflections towards (+) and away (-) from the stiffener outstand. Comparing the predicted peak bending moment in this case with the experimental result [18] shows that the present method overestimates the collapse bending moment by 5.9%. The bending moment-curvature curves for Modes 1 and 2 almost coincided. The computed peak bending moments for Modes 1 and 2 were 9.4% and 9.3% higher than the collapse bending moment.

The peak bending moments computed for these three modes of initial imperfections and the experimental collapse bending moment are summarised in Table 2. Changing the initial stiffener deflection mode from (-1/1050, +1/1950) to (-1/510, 1/510) results in a 3.3% decrease in maximum bending moment.

The hard corners in the present study are assumed to be elastic-perfectly plastic in both tension and compression. To examine the effects of alternative characteristics for these, hard corners were introduced relative to the Mode 3 specification as follows:-

Type A -the load-shortening curve of the stiffened panel adjacent to the corner;

Type B -the average compressive stress-strain curve for the plate panel alone.

Based on these assumptions, the corresponding sagging bending moment-curvature curves for the box girder were computed. The corresponding predicted maximum bending moments are listed in Table 2. Since both the stiffness and the maximum load-carrying capacity of the Mode 3 corner are greater than those of Type A, the peak bending moment is correspondingly greater. However, the difference between the two is very small (0.9%) because the plates and the stiffeners in the compression flange and webs are very stocky ($\beta=0.786$, $\lambda=0.490$).

Behaviour of the model incorporating the Type B corner lies between these two as shown in Table 2.

In most cases examined [3], behaviour of the tension elements was assumed to be elastic-perfectly plastic. To study the effects of different elemental tensile behaviour on the bending moment-curvature relationship, the elements in the tension flange were assumed to have an initial stiffness reduced due to tension yielding blocks induced by welding as given by eqn (1).

This stiffness remains constant up to yield after which it follows the perfectly plastic curve.

The corresponding peak bending moment is listed in the last column of Table 2. The effect of residual stresses in the tension flange is to decrease the initial stiffness. However, it makes little difference (1.2%) as far as the maximum bending moments are concerned.

Box Girder Models 23 and 31 [11]

A series of seven fabricated steel box girders subjected to pure bending was tested at the Technical University of Berlin by Reckling. These girders were orthogonally stiffened in a similar manner to ship's hulls. Of these, Model 23 and Model 31 were chosen for analysis. Tests on Model 31 showed that the collapse was delayed by the restraining effect of the side walls, the 'box girder effect' as described by Reckling, in spite of earlier buckling of deck panels. Model 23 had the same overall dimensions as Model 31 but had more longitudinal stiffeners in the deck and side walls. It was observed in the tests that collapse of Model 23 occurred by buckling of the plate panels between longitudinal stiffeners in the deck coinciding with failure of the whole deck.

Model 23. Component dimensions and material properties for Model 23 are given in Table 1. Its cross-section was discretised as previously described. Since only a single value of yield stress was given for the entire girder [11], this value was assumed for both the plates and the stiffeners. The welding residual stresses and initial imperfections used in the derivation of the load-shortening curves are listed in Table 3. The stiffened panels in tension were assumed to follow the material stress-strain curve, as were the hard corners in both tension and compression. These effective stress-strain curves of the structural elements were then used to generate the bending moment-curvature curves for the following cases:-

Table 3
Initial Imperfections and Comparisons between Numerical and Test Results
for Girder Models 23 and 31 [11]

	Model 23				Initial Stiffener Deflections			Model 31			Initial Plate Deflections		
	Corner Modelling		Res. Stress in Tens. Fl.		Case 1	Case 2	Case 3	Res. Stresses in Comp. Fl.		Case 4	Case 5	Case 6	Case 7
	Case 1	Case 2	Case 3	Case 4				Case 4	Case 5				
σ_r	0.20	0.20	0.20	0.20	0.20	0.20	0.20	0.05	0.35	0.20	0.20		
δ_o / b	0.25	0.25	0.25	0.25	0.55	0.55	0.55	0.55	0.55	0.22	0.88		
Δ / L	-1/1000	1/1000	-1/1000	-1/1000	1/1000	1/2000	1/500	1/1000	1/1000	1/1000	1/1000	1/1000	1/1000
	1/1000	1/1000	1/1000	1/1000	-1/1000	-1/2000	-1/500	-1/1000	-1/1000	-1/1000	-1/1000	-1/1000	-1/1000
M_o (kNm) (num)	237.9	239.9	232.8	234.6	203.0	204.3	199.7	200.1	203.0	205.9	200.3		
M_o/M_p (num)	0.887	0.895	0.868	0.875	0.800	0.806	0.788	0.789	0.800	0.812	0.790		
M_o (kNm) (exp)	249.4	249.4	249.4	249.4	215.9	215.9	215.9	215.9	215.9	215.9	215.9		
M_o/M_p (exp)	0.930	0.930	0.930	0.930	0.851	0.851	0.851	0.851	0.851	0.851	0.851		

Notes 1. Corner behaviour is represented by material stress-strain curve.
2. Unless noted, effects of residual stresses in tension flange are not considered.

1. the deck plate panels neighbouring the deck-side wall intersections were treated as hard corners;
2. additional to Case 1, the side-wall plate panels adjacent to the corners were treated as hard corners.

The predicted peak and test collapse bending moments are listed in Table 3. It can be seen that correlation between the numerical and experimental results is satisfactory as far as the maximum bending moments are concerned. The difference in the maximum values is 4.6% for Case 1, and 3.8% for Case 2. Despite this agreement, the computed bending moment-curvature curves were found to differ from the experimental curve particularly initially. Since the inclusion of welding residual stresses in the tension flange usually leads to a decrease in the initial stiffness of a box girder, two further cases were examined, viz.

3. the same as Case 1 except that residual stresses in structural elements in tension were considered;
4. the same as Case 2 except that residual stresses in structural elements in tension were considered.

The resulting peak predicted bending moments are listed in Table 3. The difference in maximum bending moment between the numerical and experimental results is 6.6% for Case 3 and 5.9% for Case 4, slightly greater than those for Cases 1 and 2, but the predicted initial stiffnesses in Cases 3 and 4 correlated significantly better with the experimental results [3].

Model 31. Component dimensions and material properties for Model 31 are given in Table 1. The model was discretised into structural elements and the stiffened panel load-shortening curves computed for the deck and side-walls having the residual stresses and initial imperfections listed for Case 1 in Table 3. These curves were then input to perform the ultimate strength analysis of the girder cross-section in which hard corners were assumed to follow the material stress-strain relationship. A 6.0% difference was found between the predicted and observed ultimate bending moments (Table 3) although the initial stiffnesses were similar.

This model was also used to examine the effects of initial stiffener deflections, weld-induced residual stress and initial plate deformation on the collapse behaviour of a girder. First the effects of initial stiffener deflection were considered. For this, in addition to Case 1 ($\Delta/L=1/1000$, $\delta_0/t=0.55$, $\sigma_r=0.20$) ultimate strength analyses were performed for the following cases:

- 2 $\Delta/L=1/2000$, $\delta_0/t=0.55$, $\sigma_r=0.20$;
- 3 $\Delta/L=1/500$, $\delta_0/t=0.55$, $\sigma_r=0.20$.

The web stiffened panels were found to be more sensitive to initial stiffener distortion than the flange panels [3].

The maximum bending moments are listed in Table 3. Not unexpectedly, the ultimate strength of Model 31 is seen to decrease with increasing initial stiffener deflection magnitude. The decrease, however, as the initial stiffener deflection varies from $\Delta/L=1/2000$ to $\Delta/L=1/500$ is only 2.2%.

The influence of weld-induced residual stresses was examined by analysing the following cases:

- 4 $\Delta/L=1/1000$, $\delta_0/t=0.55$, $\sigma_r=0.05$;
- 5 $\Delta/L=1/1000$, $\delta_0/t=0.55$, $\sigma_r=0.35$.

Although the effect of residual stresses on the stiffness and strength of the stiffened panels between Cases 1, 4 and 5 was found to be significant [3], the peak bending moments only changed by 1.5% (Table 3).

Finally, Model 31 was analysed for the following cases:

- 6 $\Delta/L=1/1000$, $\delta_0/t=0.22$, $\sigma_r=0.20$;
- 7 $\Delta/L=1/1000$, $\delta_0/t=0.88$, $\sigma_r=0.20$.

to examine the effect of initial plate deflections. The maximum predicted bending moments are listed in Table 3 from which it is seen that the ultimate strength of the box girder decreases with increases in the initial plate deflection magnitude. In particular, when the initial plate deflection varies from $\delta_0/t=0.22$ to $\delta_0/t=0.88$, the computed maximum bending moment decreases by 2.7%.

Of the cases examined above, Case 6 corresponds most closely to the tested girder so the present procedure underestimates the experimental value by 4.6%.

T.B.D. COBRA and WOLF [12]

The Torpedo-Boat Destroyer COBRA collapsed by breaking her back and sank in rough seas on her first journey in 1901. The disaster was re-examined in the light of 1980's technology [12] leading to the conclusion that since COBRA's hull was transversely framed and was structurally too weak even to withstand moderate sea conditions, the COBRA may have been lost due to buckling not being properly considered in her design. Hull strength assessments were made of T.B.D. COBRA and a similarly

constructed vessel T.B.D. WOLF in the sagging and hogging conditions using the analysis procedures reported in [19]. The results are compared below with those obtained by the present incremental moment-curvature approach.

T.B.D. COBRA. The midship cross-section of COBRA was obtained from [12] and was discretised into structural elements. The effective stress-strain curves for wide plates in compression were also taken from [12]. The ultimate strength of COBRA's hull was then evaluated using the present analysis.

Bending moment-curvature curves were derived for the sagging and hogging conditions. Compared with the maximum bending moment results of [12], a 1.3% difference was found for the sagging condition and 2.0% difference for the hogging condition. In both cases the present analysis gave the lower result.

T.B.D. WOLF. The midship cross-section of WOLF was obtained from [12]. Differences of 3.6% in maximum sagging bending moment were obtained and 1.0% in maximum hogging bending moment. The present analysis gave a lower result in the case of sagging but higher in the case of hogging.

In [3], the effect of introducing longitudinal stiffening into the hull of COBRA was examined. The results showed that the introduction of 10 longitudinal stiffeners to the existing hull led to an increase in ultimate strength of 29.6% in sagging and 21.7% in hogging. Where the frame space was increased by a factor of three and 24 stiffeners introduced, this led to a 33.3% increase in sagging ultimate strength and a 51.7% increase in hogging. For this frame space but 44 stiffeners, increases in the maximum bending moments were 65.2% and 65.1% for sagging and hogging respectively.

SIMPLIFIED SHIP BENDING STRENGTH MODEL

Introduction

The conventional approach to ship longitudinal strength calculation is based on linear bending theory. Since this makes no distinction between the tension and compression flanges, it is valid only when the compression flange is designed to resist buckling. To allow for such effects, attempts have been made to modify elementary beam theory.

As demonstrated, the present method is capable of accurately predicting the ultimate longitudinal strength of a ship's hull girder. However, it is impractical to perform such an ultimate strength analysis on a ship, particularly at the stage of preliminary design or when assessing safety levels. From these points of view, a simple expression for

the ultimate moment capacity is more helpful in assessing the margin of safety between the load-carrying capacity of the hull girder as a beam and the maximum bending moment acting on the ship.

In this section formulae are derived for predicting the ultimate bending moment capacity of a ship's hulls. Firstly, however, existing ultimate strength approaches are briefly reviewed. Simple expressions for the ultimate moment capacity are obtained from the data relating to the maximum load-carrying capacity of stiffened panels and the ultimate bending moment strength of hull girders. A design prediction procedure is then suggested and the strength formulae compared with numerical and experimental results.

Existing Strength Formulae

Excluding buckling. In [20], it was proposed that once yield stress is exceeded in either flange, the resulting excessive strain will overload the adjacent structure and hence trigger ultimate failure of the hull girder. Based on this limiting condition and linear bending theory, the ultimate bending moment M_u is given by:

$$M_u = M_y = Z \sigma_y = M_p / S_p \quad (6)$$

For the purposes of deriving explicit expressions for the ultimate moment capacity, it is convenient to represent the midship cross-section by an equivalent lumped area similar to that shown in Fig. 4 but with the stiffeners aligned with the plating. Assuming a linear stress distribution with a maximum value of σ_y in the deck, M_u for this simple box girder is [20]

$$M_u = M_y = \sigma_y AD \left[\alpha_b \gamma + 2\alpha_s \left(\frac{1}{3\gamma} - 1 + \gamma \right) + \alpha_b \left(\frac{1}{\gamma} - 2 + \gamma \right) \right] \quad (7)$$

Following the method of classical plasticity, a fully plastic condition is reached when yield stress has developed at every point throughout the depth of a girder [2]. Using the same lumped area approach, the ultimate bending moment corresponding to this limiting condition, i.e. fully plastic moment is [2]:

$$M_u = M_p = \sigma_y AD \left[\alpha_b \gamma + 2\alpha_s (1/2 - \gamma + \gamma^2) + \alpha_b (1 - \gamma) \right] \quad (8)$$

This moment represents an upper limit of a girder's longitudinal strength, but is rarely obtained due to the adverse effects of buckling and initial imperfections as demonstrated above.

Including buckling. In discussing the experimental results relating to full-scale ship structural tests, Vasta [21] suggested that the limiting bending moment for a longitudinally framed hull can be approximated by the product of its

elastic section modulus and its critical panel strength. That is, the ultimate bending moment can be taken as:

$$M_u = Z\sigma_u = (Z\sigma_y)\sigma_u/\sigma_y = M_y\phi = M_y\phi/S_r \quad (9)$$

Although the use of this simple expression was supported by the ISSC [22], it has been criticised as being pessimistic in regard to predicting ultimate strength [23] by ignoring plastic hinge capacity, and as being optimistic in respect of girder stiffness since it ignores the loss of stiffness which arises due to buckling of plates and stiffened panels. Dwight [24] has suggested that eqn (9) can be used as a lower limit for ultimate moment capacity: this is discussed later.

For the bending stress distribution corresponding to the limiting condition suggested by Vasta [21], the ultimate bending moment for a simple box girder is

$$M_u = \sigma_y AD [\alpha_s \gamma + 2\alpha_s (1/3\gamma - 1 + \gamma) + \alpha_s (1/\gamma - 2 + \gamma)] \quad (10)$$

To take buckling effects into account, Caldwell [2] considered the following limiting condition existed when the girder had reached its ultimate bending moment. In the bottom structure and the side-shells below the neutral axis, the position of which was determined by equating tension and compression zone areas, yield stress in tension was assumed to have fully developed. On the compression side, structural instability factors ϕ_b and ϕ_s were introduced for the deck and the side-shells above the neutral axis to make allowance for buckling. By using the lumped area representation of the midship cross-section, the resulting ultimate bending moment is:

$$M_u = \sigma_y AD [\phi_b \alpha_b \gamma + 2\alpha_s (1/2 - \gamma + \gamma^2 (1 + \phi_s)/2) + \alpha_s (1 - \gamma)] \quad (11)$$

As indicated in [25] it was implicit in Caldwell's approach that once an element reached its maximum load, it continued to carry that load under increasing strain. As has been seen, this is rarely the case in practice. It therefore appears to follow that eqn (11) will produce optimistic predictions of the ultimate bending moment.

In considering the buckling of plate panels under compressive loads, Oakley [26] suggested a practical approach by using the concept of an effective width of plating associated with each longitudinal stiffener. Since the effective width varies with the applied stress, this approach requires an iterative process to calculate the effective section modulus. Two or three iterations are usually needed to reach a

convergent solution [26] which gives an effective longitudinal stress distribution. The resulting ultimate bending moment is given by:

$$M_u = Z_e \sigma_y \quad (12)$$

This equation satisfies both the equilibrium the deformation condition associated with the basic assumption that plane sections remain plane, but does not allow for residual strength after the buckling of plate panels.

For a complex section, eqn (12) involves tedious iterations to determine the effective section modulus. An alternative expression has been suggested for longitudinally framed ships in the sagging condition by Mansour and Faulkner [23]:

$$M_u = Z\sigma_u(1 + kv) = (Z\sigma_y)(1 + kv)\sigma_u/\sigma_y = M_y\phi(1 + kv) = M_y\phi(1 + kv)/S_r \quad (13)$$

where k is a function of the ratio of one side-shell area to the deck area and was taken as 0.1 for a frigate cross-section in [27].

It is apparent that the ultimate bending strength of a ship's hull girder is influenced by the post-peak behaviour of its compressed members, in addition to their maximum load-carrying capacity. To include the effect of load-shedding, Wong [28] proposed two patterns of bending stress distribution. These were termed Type 1 and Type 2 for which ultimate bending moments were:

$$M_u = \sigma_y AD [\alpha_b \phi_b (\gamma_a + \gamma_b) + \alpha_s \phi_s \{ (\gamma_a^2/3)(1 + 2\zeta) + \gamma_a \gamma_b (1 + \zeta) + 2/3 \gamma_b^2 \} + 2/3 \alpha_s \gamma_c^2 + \alpha_s \gamma_c] \quad (14)$$

and

$$M_u = \sigma_y AD [\alpha_s (\phi_s/3 + 2/3 \phi_s \zeta_s + 1) \gamma^2 + \gamma (\alpha_b \zeta_b \phi_b - 2\alpha_s - \alpha_b) + \alpha_s + \alpha_b] \quad (15)$$

respectively where $\gamma_a = a/D$, $\gamma_b = b/D$ and $\gamma_c = c/D$, and a , b and c relate to extents of the assumed stress distributions. For these solutions, it is necessary to determine the load-shedding factors (ζ , ζ_b , ζ_s) to enable the ultimate strength of a girder to be calculated. It was suggested by Wong [28] that a value of 0.2 σ_u load shedding, i.e. $\zeta = 0.8$, might be used on the safe side in connection with the limit state design approach.

The ship strength model chosen for the mean ultimate moment by Faulkner and Sadden [27] was:

$$M_u = \sigma_y Z [(1 - \alpha_y + \alpha_y \alpha_c \phi) \alpha_y] \alpha_s \quad (16)$$

$$= \bar{\sigma}_y Z (1 - \alpha_y + \alpha_y \alpha_c \phi) \alpha_s$$

where $\alpha = 1 + \zeta = 1 +$ systematic errors in yield strength (subscript Y), in using idealised design codes to evaluate panel strength (c), and an allowance for redistribution following first compression failure (S). By using the systematic errors assumed in [27], eqn (16) becomes:

$$M_u = \bar{\sigma}_y Z (-0.1 + 1.4465\phi - 0.3465\phi^2) 1.15 \quad (17)$$

$$= M_p 1.15 (-0.1 + 1.4465\phi - 0.3465\phi^2) / S_f$$

Ultimate Moment Expression

It can be seen from the existing strength formulae, eqns (9,11,13,14,15, 17) that the ultimate moment capacity of a hull under vertical bending is considered to be dominated by the strength of the compression flange. Regarding this strength, Vasta [21] suggested the use of the average representative panel strength of the compression flange. This was supported by Caldwell [2] in considering the effect of structural instability. In Oakley's effective width approach [26], the panel efficiency factor is associated with plate effectiveness but makes no allowance for the strength of longitudinal stiffeners. Faulkner and Sadden [27] used the average ultimate compression strength of the critical stiffened panel.

As shown above, the ultimate bending strength of longitudinally framed hulls closely correlates with the maximum load-carrying capacity of their critical stiffened panels. Therefore, it is proposed to adopt Faulkner and Sadden's definition of panel efficiency in the derivation of a simple expression for ultimate hull strength.

The ultimate strength of a stiffened panel is primarily a function of column slenderness, plate slenderness, initial plate deformation, initial stiffener deflection, and weld-induced residual stress. However, by selecting for design, suitable values for the plate and stiffener initial deflections and residual stresses, the number of independent variables reduces to two. From Table 4-6 of [3], appropriate values for the initial imperfections seem to be:

$$\delta_o = b/200, \Delta = 0.0015L \text{ and } \sigma_r = 0.2 \sigma_y.$$

Therefore, the ultimate strength can be expressed as:

$$\phi = \sigma_u / \sigma_y = f(\lambda, \beta) \quad (18)$$

To fit a function to the numerical data contained in Table 4-6 of [3], a least-squares method was adopted. After

some preliminary investigations, eqn (18) was assumed to take the following form:

$$\phi = (C_1 + C_2 \lambda^2 + C_3 \beta^2 + C_4 \lambda^2 \beta^2 + C_5 \lambda^4)^{-0.5} \quad (19)$$

for which the least-squares solution gave the following results [3]:

$$C_1 = 0.960, C_2 = 0.765, C_3 = 0.176, C_4 = 0.131 \text{ and } C_5 = 1.046.$$

The accuracy of the predictions of eqn (19) compared with the numerical results in Table 4.6 of [3] has been assessed. The average ratio is 1.004 while the COV is 0.029.

Equation (19) is plotted in the form of $\phi - \lambda$ curves in Fig. 8, and in the form of $\phi - \beta$ curves in Fig. 9.

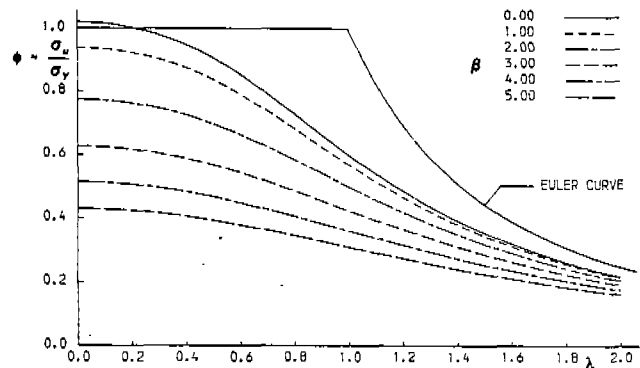


Fig. 8 Stiffened Panel Ultimate Strength versus Stiffened Panel Slenderness

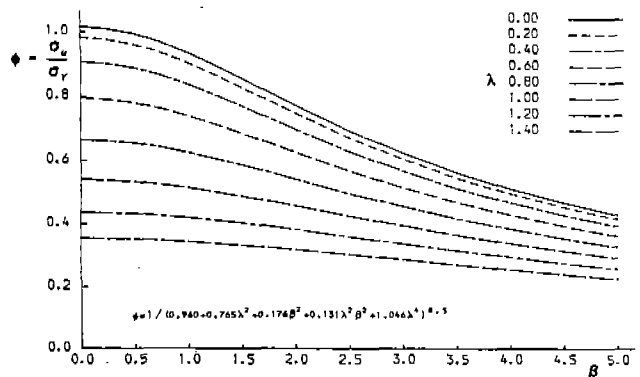


Fig. 9 Stiffened Panel Ultimate Strength versus Plate Slenderness

It can be seen in these figures that eqn (19) gives 1.021 when λ and β equal zero. Theoretically it should be unity, but if an allowance is made for the difference between tensile and compressive yield, and yield stress is determined from tensile tests while compression failure is the mode under consideration, this would be the form of modification required. Thus, since eqn (19) provides a good estimate for all other λ and β , it seems reasonable to

retain the equation as derived since it makes a small concession to the extra strength demonstrated by compressive yielding.

The ultimate moment capacity of longitudinally framed hulls under vertical bending closely correlates with the ultimate strength of the critical compression panel, as demonstrated in Fig. 10 and Table 4 for girders in sagging, and in Fig. 11 and Table 4 for girders in hogging. Since many hard corners are provided by the keel plates, deep girders and bilge keels which exist in the compressed part of a vessel in hogging, it is necessary to consider sagging and hogging conditions separately in deriving simple expressions for the ultimate moment capacity.

In the sagging condition, all of the longitudinally framed girders analysed above and in [3] are included in Fig. 10 and Table 4 except for HULL B (composite girder), Type 1 COBRA (mixed framing), Type 2 COBRA (mixed framing) and TYPE 14 Class (relatively small deck area). The numerical results for the TYPE 81 and LEANDER Class hulls were derived without superstructures.

The relationship between hull ultimate moment and stiffened panel strength was assumed to take the following form:

$$M_u / M_p = d_1 + d_2 \phi + d_3 \phi^2 \quad (20)$$

where panel strength is obtained from eqn (19). Using least-squares [3], the

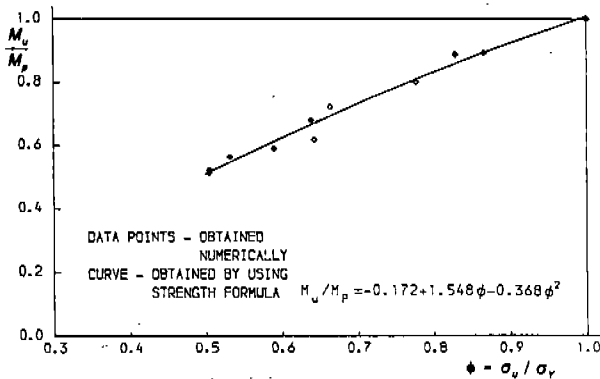


Fig. 10 Ultimate Bending Moment v Critical Stiffened Panel Strength for Hulls in Sagging

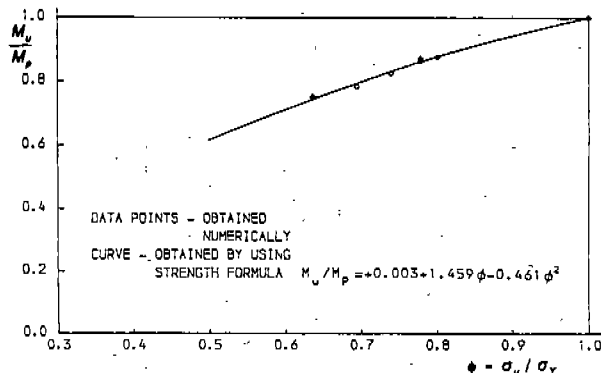


Fig. 11 Ultimate Bending Moment v Critical Stiffened Panel Strength for Hulls in Hogging

Table 4
Comparison of Numerical, Experimental and Predicted Bending Strengths for Girders in Sagging and Hogging

Ship or Girder Model	Critical Stiffened Panel		Ultimate Bending Mom.			M_u / M_p Ratios		
	λ	β	ϕ	num.	expt.	eqn(*)	eqn(*)	
			eqn(19)					
Sagging eqn (*) = eqn (21)								
Model 2	0.644	1.873	0.664	0.722	0.689	0.694	0.961	1.007
Model 4	0.490	0.786	0.866	0.892	0.842	0.893	1.001	1.060
Model 23	0.465	1.173	0.829	0.887	0.930	0.859	0.968	0.924
Model 31	0.396	1.673	0.777	0.800	0.851	0.809	1.011	0.951
Hull A	0.598	2.204	0.639	0.680	-	0.667	0.981	-
Cobra - Type 3	0.769	2.073	0.590	0.591	-	0.613	1.037	-
Whitby Class	0.466	3.666	0.505	0.514	-	0.516	1.004	-
Rothsay Class	0.466	3.666	0.505	0.524	-	0.516	0.985	-
Type 81 Class	0.509	2.376	0.643	0.619	-	0.671	1.084	-
Leander Class	0.765	1.925	0.532	0.564	-	0.547	0.971	-
						Mean	1.000	0.986
						COV	0.037	0.060
Hogging eqn (*) = eqn (22)								
Cobra - Type 3	0.650	2.073	0.637	0.751	-	0.745	0.992	-
Type 14 Class	0.548	1.582	0.741	0.825	-	0.831	1.007	-
Whitby Class	0.408	1.633	0.780	0.863	-	0.860	0.996	-
Rothsay Class	0.408	1.633	0.780	0.870	-	0.860	0.988	-
Type 81 Class	0.385	2.232	0.695	0.784	-	0.788	1.005	-
Leander Class	0.413	1.481	0.802	0.875	-	0.877	1.002	-
						Mean	0.998	
						COV	0.008	

constants in eqn (20) were found as:

$$M_u/M_p = -0.172 + 1.548\phi - 0.368\phi^2 \quad (21)$$

In the hogging condition, all box girder models, HULL A (relatively weak bottom structure) and HULL B (composite girder) were excluded from the derivation and hence are not included in Fig. 11 or Table 4. The TYPE 81 and LEANDER Class hulls were again treated as hulls without superstructure in deriving the numerical results. By similarly using least-squares the following expression was obtained [3]:

$$M_u/M_p = 0.003 + 1.459\phi - 0.461\phi^2 \quad (22)$$

Equations (21) and (22) demonstrate that the ultimate bending moment is a function of the fully plastic moment and the ultimate strength of the critical stiffened panel. To predict the ultimate longitudinal strength for a hull girder or box girder, the following procedure is suggested:

1. Determine the plastic neutral axis position, i.e. the interface that divides the cross-section into two regions with equal squash loads in compression and tension.
2. Calculate the fully plastic moment of the fully effective midship section.
3. Identify the critical stiffened panel. Initially, this can be selected as the panel appearing most frequently in the compression flange of the girder in either the sagging or hogging condition. More rigorously, the strength of several panels can be evaluated and the weakest one identified.
4. Compute the values of the column slenderness λ and the plate slenderness β for the critical panel.
5. Calculate the ultimate strength ϕ of the critical panel by using eqn (19).
6. Calculate the ultimate bending moment for the girder by using eqn (21) or (22).

Comparisons with Numerical and Existing Predictions

The results of applying the above procedure to the vessels under consideration are compared with those obtained numerically in Fig.10 (sagging) and Fig. 11 (hogging): Table 4 summarises these results. The agreement is seen to be satisfactory, with a mean of 1.000 and COV = 0.037 in sagging and a mean of 0.998 and COV = 0.008 in hogging being obtained for the ratio of the predictions to the numerical results. Even the predictions of the experimental results are good as shown in Table 4 where the

mean for the girders in sagging is 0.986 with a COV of 0.060.

The predictions of the existing strength formulae for ultimate moment capacity reviewed above are compared with the numerical results in Table 5 for both the sagging and hogging conditions. Since the effective width approach requires an iterative process to calculate the effective section modulus, it is excluded from the comparisons. In view of the uncertainty concerning the load-shedding factor in Wong's formulae, these are also excluded.

It was suggested in the review that Vasta's approach would be pessimistic when predicting ultimate hull strength since it ignored plastic hinge capacity. This seems to be confirmed in Table 5 where it is seen that a mean of 0.815 and a COV = 5.7% for sagging and a mean of 0.776 and a COV = 1.7% for hogging are obtained for the ratio of Vasta's prediction to the numerical result.

The review also suggested that since the effect of load-shedding is not allowed for in Caldwell's approach, eqn (11) is likely to produce optimistic predictions of the ultimate bending moment. This is clearly demonstrated in Table 5.

Since Mansour and Faulkner's expression eqn (13) gives a mean compared with the numerical result of 0.897 and COV = 0.057 (sagging) and a mean of 0.854 and COV = 0.017 (hogging), this approach achieves an improvement over that of Vasta but with the same COV.

Faulkner and Sadden's expression, eqn (17), is seen to improve both the mean (0.995) and the COV (0.052) in sagging and to improve the mean (0.941) with a small COV (0.020) in hogging, and clearly is the best of the existing formulae. Compared with the present approach, it still generates larger values of COV (0.052 and 0.020) compared with 0.037 and 0.008 for hulls in sagging and hogging respectively while still needing more calculations including some estimates of systematic errors.

RELIABILITY MODELLING AND ANALYSIS

Background

The work of ISSC'91 Committee V.1 involves the reliability analysis of a floating production vessel and the attendant wave load and structural analyses [29]. Both conventional linear and more innovative non-linear solutions to the wave-induced moments were determined. Comparisons with measurements on the vessel concerned enabled the accuracy of these results to be quantified stochastically for use in the reliability analysis. The following

Table 5
Comparison of Present Numerical and Predicted Bending Strengths
for Girders in Sagging and Hogging

Ship or Girder Model	Ultimate Bending Moment M_u / M_p					M_u / M_p Ratios			
	Present	Vasta	Caldwell	Mansour	Faulkner	(2)	(3)	(4)	(5)
	Num. (1)	[21] (2)	[2] (3)	[23] (4)	[27] (5)	(1)	(1)	(1)	(1)
Sagging									
Model 2	0.722	0.626	0.840	0.689	0.768	0.867	1.163	0.954	1.064
Model 4	0.892	0.722	0.924	0.794	0.856	0.809	1.036	0.890	0.960
Model 23	0.887	0.747	0.940	0.822	0.892	0.842	1.060	0.927	1.006
Model 31	0.800	0.700	0.880	0.770	0.844	0.875	1.100	0.963	1.055
Hull A	0.680	0.586	0.758	0.645	0.720	0.862	1.115	0.949	1.059
Cobra - Type 3	0.591	0.464	0.760	0.511	0.573	0.785	1.286	0.865	0.970
Whitby Class	0.514	0.402	0.666	0.443	0.497	0.782	1.296	0.862	0.967
Rothsay Class	0.524	0.401	0.670	0.441	0.495	0.765	1.279	0.842	0.945
Type 81 Class	0.619	0.510	0.768	0.560	0.626	0.824	1.241	0.905	1.011
Leander Class	0.564	0.418	0.727	0.459	0.516	0.741	1.289	0.814	0.915
					Mean	0.815	1.186	0.897	0.995
					COV	0.057	0.087	0.057	0.052
Hogging									
Cobra - Type 3	0.751	0.574	0.850	0.631	0.705	0.764	1.132	0.840	0.939
Type 14 Class	0.825	0.640	0.877	0.704	0.777	0.776	1.063	0.853	0.942
Whitby Class	0.863	0.663	0.914	0.729	0.799	0.768	1.059	0.845	0.926
Rothsay Class	0.870	0.666	0.920	0.733	0.803	0.766	1.057	0.842	0.923
Type 81 Class	0.784	0.626	0.827	0.689	0.765	0.798	1.055	0.879	0.976
Leander Class	0.875	0.685	0.933	0.754	0.823	0.783	1.066	0.862	0.941
					Mean	0.776	1.072	0.854	0.941
					COV	0.017	0.028	0.017	0.020

is a summary of this activity emphasising those parts relevant to the simple hull girder modelling discussed above.

For the reliability analysis, a second-order procedure was used. This was described in the ISSC'88 Report of this Committee [30] but it has since been enhanced with an 1989 release [31] in which it is possible to evaluate the parametric sensitivity of the reliability index to any parameter at the "failure point" in the basic variable space. This option is used to assess the influence of the model uncertainty parameters and of other parameters contained in the failure equations. This particular software also has the capability to generate an improve second-order solution through simulation about the failure point in the independent standard normal space.

Failure equation and stochastic modelling

For this case, the failure equation is

$$\chi_u M_u - \chi_{MC} M_w - \psi_s \chi_{sw} M_{sw} \geq 0 \quad (23)$$

The adopted stochastic modelling involves 12 variables which are listed together with their distribution functions in Table 6.

The stochastic modelling for each of the variables was chosen as follows:

- σ_y derived from DnV material certificates which gave good agreement with existing data;
- E in accordance with previous ISSC work [30];

- L, t, b geometric variables, modelled as in [30];
- M_u using non-linear theory (see Chapter 2 of [29]), the adopted extreme value distribution is Gumbel, the parameters for which have been derived on the basis of time simulations of "long-term equivalents" to short-term seas states;
- M_{sw} the Rayleigh distribution closely fits the still water extreme bending moment distribution as demonstrated in [32] which present data pertaining to the analysed vessel. The most important non-linear effect in the response is that of the buoyancy force which manifests itself as the difference between hogging and sagging.
- χ_u this value is assessed by means of experimental - calculation comparisons.

Table 6
Variable Stochastic Modelling

Var.	Dist. Type	Mean Value	COV	Ref.
σ_y	Lognormal	407.5*	0.066	
E	Normal	210,000	0.050	[30]
L	Normal	3700	0.04	
t	Normal	13.5	0.04	
b	Normal	690	0.04	
M_u	Gumbel	3693	0.133	
M_{sw}	Rayleigh	326.7	0.52	[32]
χ_u	Normal	1.0	0.15	
χ_{MC}	Normal	0.90	0.15	[33]
χ_{sw}	Normal	1.0	0.05	
r	Normal	79.5	0.04	

* for the plating

Taking the inverses of the values presented in Table 4, the bias is 1.018 and COV is 0.061. Because the tests involved a small number of laboratory experiments on steel box girders, these were felt to be not necessarily fully representative of ships girders so the COV was increased to 0.15, a compromise between the derived value and that of 0.20 suggested in [34].

- χ_{MC} this has been evaluated from an analysis of full scale data relating to the selected vessel. The factor accounts for the uncertainties arising from spectral representation and from the shape of the transfer function which is usually predicted using linear strip theory. The model uncertainty, normally distributed with a bias of 0.90 and COV of 0.15 is in good agreement with the formulation in [33]

$$\text{Bias} = -0.0050\theta - 0.42V + 0.70C_p + 1.25$$

$$90 \leq \theta \leq 180 \quad (24)$$

$$\text{Bias} = -0.0063\theta + 1.22V + 0.66C_p + 0.06$$

$$0 \leq \theta \leq 90$$

and a standard deviation of 0.12. Equations (24) have been determined by a systematic comparison between theoretical and experimental results.

- χ_{sw} due to the large amount of available data [32], it should be quite small, however, it is increased because of the Rayleigh fit to the extreme value distribution.

- r taken as geometry variable while actually a function of a number of such entities.

Results and Comments

The results of the reliability analysis are presented in Table 7.

From Table 7 it is seen that the reliabilities determined by the first- (I) and second-order (II) methods are similar and that simulation (III) does not improve on these estimates despite evidence [29] that the failure surface is multi-modal. Modelling of radius of gyration was introduced to help reduce the impact of the multiple failure surface on the solution.

In the panel strength modelling approach [3], the stiffened panel is considered as adjacent half panels with alternate modes of initial deformation. Thus strength is controlled by the combined failing of the plate in one panel and the stiffener in the other. The stiffened panel response is initially governed by loss of stiffness in the initially distorted plating but strength is then usually limited by the onset of

Table 7
Hull Girder Reliability Analysis

Var.	Mean	Failure Point	Sens. Factors	Partial Factors
σ_y	407.5*	415.1	0.101	1.019
E	210000	207750	-.078	0.989
M_w	3693	4548	.567	1.232
M_{sw}	326.7	329	.052	1.007
L	3700	3724	.058	1.006
t	13.5	13.4	-.065	0.993
b	690	695	.064	1.007
χ_u	1.00	0.810	-.686	0.810
χ_{MC}	0.90	1.055	.417	1.172
χ_{sw}	1.00	1.00	-	1.000
r	79.5	77.5	-.058	0.975
β_I		2.765		
β_{II}		2.667		
β_{III}		2.608		

* for the plating

yield at the stiffener tip. In [3], and thus in the present study, it was assumed that yield stress in both the plate and the stiffener was the same. The effects of different yield stresses have not been examined. Presumably however as average value might be more appropriate for the type of analysis conducted here.

Parametric sensitivities were evaluated for a limited range of the variables. Those considered and the results achieved are listed in Table 8.

Table 8
Parametric Sensitivity Factors

Parameter	Sensitivity Factors
σ_y	0.004
Mean χ_u	4.574
s.d. χ_u	-8.676
Mean χ_{MC}	-3.088
s.d. χ_{MC}	-3.560
Mean χ_{sw}	0.095
s.d. χ_{sw}	-0.001
ψ	-0.001

From the table it is seen that modelling accuracy dominates, i.e. the accuracy of the predictions relative to measurements from a strength as well as a loading point of view are most critical.

CONCLUSION

A numerical procedure for the determination of ship girder longitudinal bending strength is described. It accounts for the primary variables affecting strength, namely, yielding and

plate and stiffened panel slendernesses, and the secondary contributors of initial deflections and welding residual stresses. Comparisons are presented with experimental results which demonstrate its accuracy.

For preliminary design and reliability analysis modelling, a simplified model is developed based on the observation that ship bending strength correlates closely with the critical stiffened panel strength. The process for identifying the critical panel is described and comparisons with the experimental and numerical work demonstrate its accuracy. The model is then subjected to reliability analysis as part of the ISSC'91 studies.

ACKNOWLEDGEMENT

The ISSC work reported here was executed by RINA under the direction of Dr M Dogliani.

REFERENCES

1. ISSC, "Report of Committee 10", Proc. Vol 2, International Ship Structures Congress, Oslo, 1967.
2. Caldwell, J B, "Ultimate Longitudinal Strength", Trans. RINA, Vol 107, 1965.
3. Lin, Y-T, "Ship Longitudinal Strength Modelling", PhD Thesis, University of Glasgow, 1985.
4. Valsgard, S, "Ultimate Capacity of Plates in Transverse Compression", Det norske Veritas, Report No 79-0104, 1979.
5. Dier, A F and Dowling, P J, "The Strength of Plates subjected to Biaxial Forces", in Behaviour of Thin-Walled Structures, Ed. J Rhodes and J Spence, Elsevier Applied Science, London, 1984.
6. Frieze, P A, Dowling, P J and Hobbs, R E, "Ultimate Load Behaviour of Plates in Compression", in Steel Plated Structures, Ed. P J Dowling, J E Harding and P A Frieze, Crosby Lockwood Staples, London, 1977.
7. Little, G H, "Stiffened Steel Compression Panels - Theoretical Failure Analysis", The Structural Engineer, Vol 54, No 12, Dec. 1976.
8. Smith, C S, "Influence of Local Compressive Failure on Ultimate Longitudinal Strength of a Ship's Hull", International Symposium on Practical Design in Shipbuilding, PRADS, Tokyo, Oct. 1977.
9. Dowling, P J et al, "Experimental and Predicted Collapse Behaviour of Rectangular Steel Box Girders", Proc. International Conf. Steel Box Girder Bridges, ICE, London, Feb. 1973.
10. Dowling, P J, Moolani, F M and Frieze, P A, "The Effect of Shear Lag on the Ultimate Strength of Box Girders", in Steel Plated Structures, Ed. P J Dowling, J E Harding and P A Frieze, Crosby Lockwood Staples, London, 1977.
11. ISSC "Report of Committee II.2 on Non-Linear Structural Response", 7th International Ship Structures Congress, Paris, 1979.
12. Faulkner, J A et al, "The Loss of HMS COBRA - A Reassessment", Spring Meetings, RINA, London, 1984.
13. Guile, P J D and Dowling, P J, "Steel Box Girders, Model 2 - Progress Report 1", Engg Structures Laboratory, Imperial College, London, Nov. 1971.
14. Frieze, P A and Dowling, P J, "Steel Box Girders, Model 2 - Progress Report 2", Engg Structures Laboratory, Imperial College, London, June, 1972.
15. Chatterjee, S and Dowling, P J, "Steel Box Girders, Model 2 - Progress Report 3", Engg Structures Laboratory, Imperial College, London, May, 1972.
16. Guile, P J D and Dowling, P J, "Steel Box Girders, Model 4 - Progress Report 1", Engg Structures Laboratory, Imperial College, London, Feb., 1972.
17. Moolani, F M and Dowling, P J, "Steel Box Girders, Model 4 - Progress Report 2", Engg Structures Laboratory, Imperial College, London, March, 1972.
18. Chatterjee, S and Dowling, P J, "Steel Box Girders, Model 4 - Progress Report 3", Engg Structures Laboratory, Imperial College, London, June, 1972.
19. Smith, C S, "Structural Redundancy and Damage Tolerance in Relation to Ultimate Ship Hull Strength", Proc. Symposium on Design, Inspection and Redundancy, Williamsburg, 1983.
20. Evans, J H, Discussion of ref. 2.
21. Vasta, J, "Lessons Learned from Full Scale Structural Tests", Trans. SNAME, Vol 66, 1958.
22. ISSC, "Report of Committee on Plastic and Limit Analysis", International Ship Structures Congress, Tokyo, 1970.
23. Mansour, A E and Faulkner, D, "On Applying the Statistical Approach to Extreme Sea Loads and Ship Hull Strength", Trans. RINA, Vol 115, 1973.
24. Dwight, J B, "Collapse of Steel Compression Panels", in Developments in Bridge Design and Construction, Crosby Lockwood, London, 1971.
25. Faulkner, D, Discussion of ref. 2.
26. Oakley, O H, Discussion of ref. 21.
27. Faulkner, D and Sadden, J A, "Towards a Unified Approach to

- Ship Structural Safety", Trans. RINA, Vol 121, 1979.
28. Wong, Y L, "Some Considerations in the Ultimate Strength of Ships", MSc Thesis, University of Glasgow, 1977.
 29. ISSC, "Report of Committee V.1 - Applied Design", International Ship and Offshore Structures Congress, Wuxi, 1991.
 30. ISSC, "Report of Committee V.1 - Applied Design", International Ship and Offshore Structures Congress, Copenhagen, 1988.
 31. Gollwitzer, S, Guers, F and Rackwitz, R, "SORM (Second-Order Reliability Method) Manual", Release 1989.
 32. Moan, T and Jiao, G, "Characteristic Still Water Effects for Production Ships", University of Trondheim, December 1988.
 33. Guedes Soares, C and Moan, T, "Uncertainty Analysis and Code Calibration on the Primary Load Effects in Ship Structures", ICOSSAR'85, 4th International Conference on Structural Safety and Reliability.
 34. Faulkner, D, Oral Discussion to Report of ISSC'88 Committee V.1, Lyngby, August, 1988.

DISCUSSION

Y.N. Chen

Paul, I just wanted to make a point of clarification. The partial factors that you obtained, are they applicable to the mean value or are they some kind of design value?

P.A. Frieze

The partial factors listed in the paper are the traditional ones extracted from FORM techniques. They, therefore, represent the "failure" or "design" point value divided by the mean value of the variable concerned.